

SUPPLEMENTAL MATERIAL

Jeng et al., <http://dx.doi.org/10.1085/jgp.201611651>

wild-type TMEM16A (WT•WT)

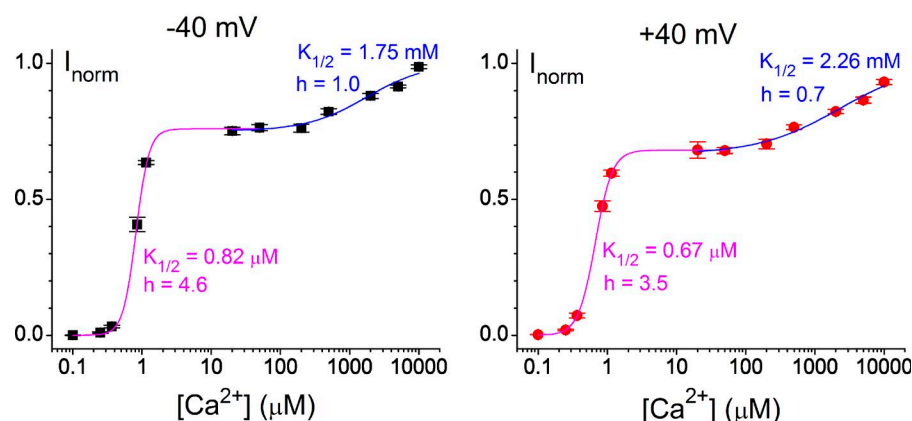


Figure S1. **Dose-response curves of the wild-type TMEM16A channel (WT•WT) from 0.1 μM to 10 mM $[\text{Ca}^{2+}]$.** Left and right panels show data obtained at -40 and $+40$ mV, respectively. Data points (mean \pm SEM) were obtained by normalizing the Ca^{2+} -activated currents at each $[\text{Ca}^{2+}]$ to those obtained at 20 mM. Solid curves are drawn according to the curve fitting of data points to the Hill equation in two concentration ranges: high-affinity range (0.1–50 μM , magenta curves) and low-affinity range (20 μM to 20 mM, blue curves). In fitting data points from 0.1 to 50 μM (the high-affinity range), the maximal I_{norm} was set as a free parameter for curve fitting while the minimal value of I_{norm} was 0. The fitted saturated I_{norm} values at -40 and $+40$ mV in this high-affinity region were 0.759 and 0.681, respectively. For the curve fitting in the low-affinity region, the minimal I_{norm} was set as a free parameter while the saturated I_{norm} was 1. The fitted minimal I_{norm} values for data at -40 and $+40$ mV were 0.751 and 0.666, respectively. The $K_{1/2}$ and the Hill coefficient, h , of each dose-response curve are depicted next to the curve.

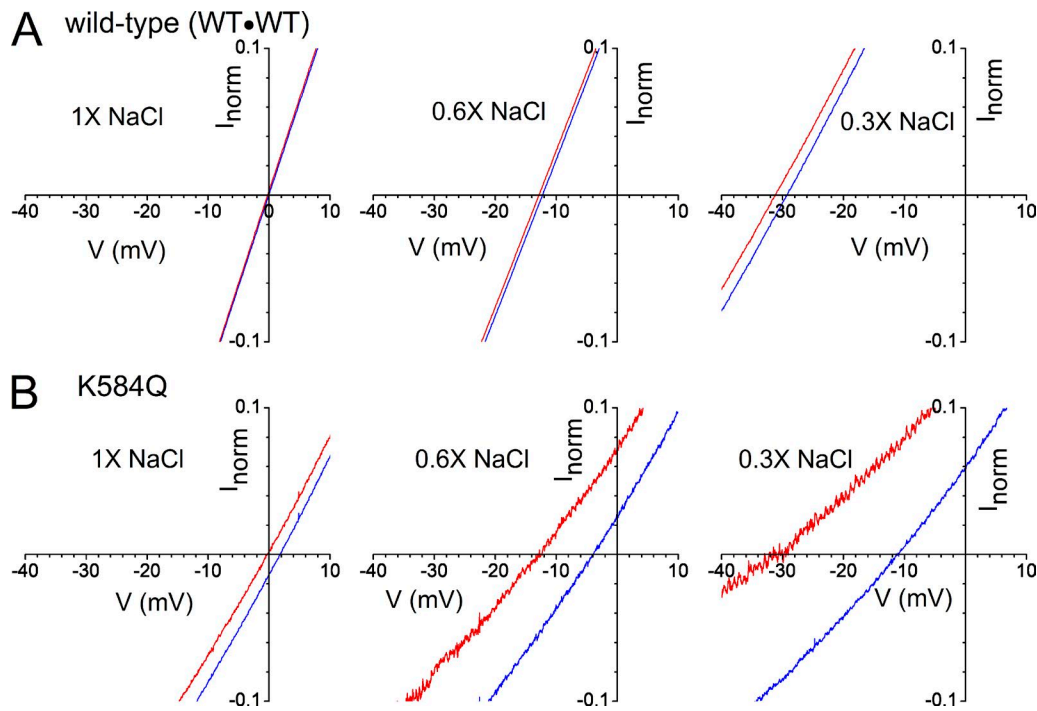


Figure S2. **Precisions of E_{rev} measurements are affected by leak current subtraction.** (A) Wild-type TMEM16A (WT•WT). (B) K584Q mutant. In both panels, current traces with and without leak subtraction are colored in red and blue, respectively. Recording traces were obtained with $1\times [\text{NaCl}]_o$ (140 mM) and indicated $[\text{NaCl}]_i$ in each panel. Four and seven normalized I-V curves of the wild-type channel and the K584Q mutant, respectively, were averaged. The SEM for each averaged I-V curve is not shown. The leak-subtracted traces in $1\times [\text{NaCl}]_i$ are the same as those shown in Fig. 7 C (left). Notice that E_{rev} is shifted to more depolarized voltage without subtraction of the I-V curve obtained in $0 [\text{Ca}^{2+}]$. The effect of the endogenous current on the E_{rev} of the wild-type channel was small (only ~ 2 mV in the worst case of $0.3\times [\text{NaCl}]_i$). In contrast, the shift of E_{rev} was significant in the K584Q mutant because the expression of this mutant was much worse than that of the wild-type channel. Furthermore, the I-V curve of K584Q is outwardly rectified, and the rectification effect was further amplified by reducing $[\text{NaCl}]_i$ (see Fig. 6 A), leading to a small ratio of channel conductance/leak conductance. Thus, without leak subtraction, the more reduction of $[\text{NaCl}]_i$, the greater the error of E_{rev} .

Table S1. **Reversal potentials in millivolts (mean \pm SEM) for the wild-type TMEM16A channel and various channel constructs harboring the K584Q mutation**

Channel constructs	$[\text{NaCl}]_i = 140 \text{ mM } (1\times)$	$[\text{NaCl}]_i = 84 \text{ mM } (0.6\times)$	$[\text{NaCl}]_i = 42 \text{ mM } (0.3\times)$
WT•WT ($n = 4$)	-0.5 ± 0.5	-13.0 ± 0.4	-31.5 ± 0.3
K584Q ($n = 7$)	-0.4 ± 0.4	-13.1 ± 0.5	-31.4 ± 0.5
E698C(K584Q)-WT ($n = 4$)	-0.3 ± 0.3	-12.0 ± 0.4	-30.8 ± 0.5
E698C-WT ($n = 4$)	-1.2 ± 0.5	-13.3 ± 0.5	-31.0 ± 0.9
E698C-WT(K584Q) ($n = 4$)	-0.8 ± 0.3	-13.0 ± 1.0	-32.5 ± 0.3

$[\text{NaCl}]_o = 140 \text{ mM}$. $[\text{Ca}^{2+}]_i = 20 \text{ }\mu\text{M}$.